High average power mode-locked figure-eight Yb fibre master oscillator

Y. S. Fedotov, A.V. Ivanenko, S. M. Kobtsev,* and S. V. Smirnov

Division of Laser Physics and Innovative Technologies, Novosibirsk State University, Pirogova str., 2, Novosibirsk, 630090, Russia

kobtsev@lab.nsu.ru

Abstract: For the first time, we demonstrate the possibility to generate record-high output radiation power exceeding 1 W in an all-fibre figure-eight mode-locked Yb fibre master oscillator based on non-linear amplifying loop mirror. Generated at the repetition rate of 25 MHz clusters of sub-pulses with duration of no more than 200 fs have envelope width of 23 ps or less. Two typical mode-locked laser regimes with substantially different generation spectra are identified and results of their study presented. Numerical modelling of laser generation in the proposed layout agrees well with the measured experimental data.

OCIS codes: (140.3510) Lasers, fiber; (060.4370) Nonlinear optics, fibers; (140.4050) Mode-locked lasers; (320.7090) Ultrafast lasers.

References and links

1. N. J. Doran and D. Wood, "Nonlinear-optical loop mirror," Opt. Lett. **13**(1), 56–58 (1988).
2. M. E. Fermann, F. Haberl, M. Hofer, and H. Hochreiter, "Nonlinear amplifying loop mirror," Opt. Lett. **15**(13), 752–754 (1990).
3. G. W. Pearson, R. Zanoni, and J. S. Krasinski, "Analysis of ultra-short pulse propagation in a fiber nonlinear amplifying loop mirror," Opt. Commun. **103**(5–6), 507–518 (1993).
4. M. E. Fermann, "Ultrafast Fiber Oscillators," in *Ultrafast Lasers: Technology and Applications*, M. E. Fermann A. Galvanauskas, and G. Sucha, eds. (CRC Press, 2002), Chap. 3.
5. M. Salhi, F. Amrani, H. Leblond, and F. Sanchez, "Analytical investigation of a figure-eight single-pulse all-fiber laser based on a nonlinear amplifying loop mirror," Phys. Rev. A **82**(4), 043834 (2010).
6. K. Ozgören, B. Öktem, S. Yılmaz, F. Ö. Ilday, and K. Eken, "83 W, 3.1 MHz, square-shaped, 1 ns-pulsed all-fiber-integrated laser for micromachining," Opt. Express **19**(18), 17647–17652 (2011).
7. M. A. Chernysheva, A. A. Krylov, P. G. Kryukov, and E. M. Dianov, "Nonlinear amplifying loop-mirror-based mode-locked Thulium-doped fiber laser," IEEE Photon. Technol. Lett. **24**(14), 1254–1256 (2012).
8. P. Polynkin, A. Polynkin, D. Panasenko, N. Peyghambarian, M. Mansuripur, and J. Moloney, "All-fiber passively mode-locked laser oscillator at 1.5 μm with watts-level average output power and high repetition rate," Opt. Lett. **31**(5), 592–594 (2006).
9. N. H. Seong, D. Y. Kim, and S. P. Veetil, "Mode-locked fiber laser based on an attenuation-imbalanced nonlinear optical loop mirror," Opt. Commun. **280**(2), 438–442 (2007).
10. X. H. Li, Y. S. Wang, W. Zhao, W. Zhang, Z. Yang, X. H. Hu, H. S. Wang, X. L. Wang, Y. N. Zhang, Y. K. Gong, C. Li, and D. Y. Shen, "All-normal dispersion, figure-eight, tunable passively mode-locked fiber laser with an invisible and changeable intracavity bandpass filter," Laser Phys. **21**(5), 940–944 (2011).
11. J. Li, Z. Zhang, Z. Sun, H. Luo, Y. Liu, Z. Yan, C. Mou, L. Zhang, and S. K. Turitsyn, "All-fiber passively mode-locked Tm-doped NOLM-based oscillator operating at 2-μm in both soliton and noisy-pulse regimes," Opt. Express **22**(7), 7875–7882 (2014).
12. I. N. Duling III, C.-J. Chen, P. K. A. Wai, and C. R. Menyuk, "Operation of a nonlinear loop mirror in a laser cavity," IEEE J. Quantum Electron. **30**(1), 194–199 (1994).
13. M. Horowitz, Y. Barad, and Y. Silberberg, "Noiselike pulses with a broadband spectrum generated from an erbium-doped fiber laser," Opt. Lett. **22**(11), 799–801 (1997).
14. S. Kobtsev, S. Kukarin, S. Smirnov, S. Turitsyn, and A. Latkin, "Generation of double-scale femto/pico-second optical lumps in mode-locked fiber lasers," Opt. Express **17**(23), 20707–20713 (2009).
15. B. Nie, G. Parker, V. V. Lozovoy, and M. Dantus, "Energy scaling of Yb fiber oscillator producing clusters of femtosecond pulses," Opt. Eng. **53**(5), 051505 (2014).
16. Y. S. Fedotov, S. M. Kobtsev, R. N. Arif, A. G. Rozhin, C. Mou, and S. K. Turitsyn, "Spectrum-, pulsewidth-, and wavelength-switchable all-fiber mode-locked Yb laser with fiber based birefringent filter," Opt. Express **20**(16), 17797–17805 (2012).

#225384 - $15.00 USD Received 21 Oct 2014; accepted 17 Nov 2014; published 11 Dec 2014

17. A. B. Grudinin, D. N. Payne, P. W. Turner, L. J. Nilsson, M. N. Zervas, M. Ibsen, and M. K. Durkin, "Multi-fibre arrangements for high power fibre lasers and amplifiers," Patent US 6826335 B1, issued date: Nov 30, (2004).
18. A. V. Ivanenko, S. M. Kobtsev, S. V. Kukarin, and A. S. Kurkov, "Femtosecond Er laser system based on side-coupled fibers," Laser Phys. **20**(2), 341–343 (2010).
19. S. Smirnov, S. Kobtsev, S. Kukarin, and A. Ivanenko, "Three key regimes of single pulse generation per round trip of all-normal-dispersion fiber lasers mode-locked with nonlinear polarization rotation," Opt. Express **20**(24), 27447–27453 (2012).
20. X. H. Li, Y. S. Wang, W. Zhang, W. Zhao, X. H. Hu, Z. Yang, C. X. Gao, X. L. Wang, X. L. Liu, D. Y. Shen, and C. Li, "Low-repetition-rate Ytterbium-doped fiber laser based on a CFBG from large anomalous to large normal dispersion," Laser Phys. **21**(12), 2112–2117 (2011).
21. A. F. Runge, C. Aguergaray, N. G. Broderick, and M. Erkintalo, "Raman rogue waves in a partially mode-locked fiber laser," Opt. Lett. **39**(2), 319–322 (2014).
22. O. G. Okhotnikov and F. M. Araújo, "Cavity dumping of fiber lasers by phase-modulated optical loop mirrors," Opt. Lett. **21**(1), 57–58 (1996).
23. S. Kobtsev, S. Smirnov, S. Kukarin, and S. Turitsyn, "Mode-locked fiber lasers with significant variability of generation regimes," Opt. Fiber Technol. **20**(6), 615–620 (2014).
24. S. V. Smirnov, S. M. Kobtsev, and S. V. Kukarin, "Efficiency of non-linear frequency conversion of double-scale pico-femtosecond pulses of passively mode-locked fiber laser," Opt. Express **22**(1), 1058–1064 (2014).
25. S. Kobtsev, S. Kukarin, S. Smirnov, and I. Ankudinov, "Cascaded SRS of single- and double-scale fiber laser pulses in long extra-cavity fiber," Opt. Express **22**(17), 20770–20775 (2014).
26. R. R. Gattass and E. Mazur, "Femtosecond laser micromachining in transparent materials," Nat. Photonics **2**(4), 219–225 (2008).
27. S. Nolte, S. Döring, A. Ancona, J. Limpert, and A. Tünnermann, "High repetition rate ultrashort pulse micromachining with fiber lasers," in Advances in Optical Materials, OSA Technical Digest (CD) (Optical Society of America, 2011), paper FThC1.
28. M. Erdoğan, B. Öktem, H. Kalaycıoğlu, S. Yavaş, P. K. Mukhopadhyay, K. Eken, K. Ozgören, Y. Aykaç, U. H. Tazebay, and F. Ö. Ilday, "Texturing of titanium (Ti6Al4V) medical implant surfaces with MHz-repetition-rate femtosecond and picosecond Yb-doped fiber lasers," Opt. Express **19**(11), 10986–10996 (2011).
29. M. Murakami, B. Liu, Z. Hu, Z. Liu, Y. Uehara, and Y. Che, "Burst-mode femtosecond pulsed laser deposition for control of thin film morphology and material ablation," Appl. Phys. Express **2**, 042501 (2009).

1. Introduction

Figure-eight (F8) fibre lasers [1–4] offer a practically interesting configuration of ring lasers, where passive mode locking may be achieved without resorting to the effect of non-linear polarisation evolution (NPE), saturable absorbers, or end reflectors (used in linear cavities). This possibility is attractive because the effect of NPE requires continuous high-precision control over the radiation polarisation, saturable absorbers, as a rule, have limited lifetime compared to other components of a fibre laser cavity, whereas end reflectors must have a relatively broad reflection spectrum exceeding that of the generated short pulses, which poses certain problems in all-fibre laser systems.

Mode-locked F8 fibre master oscillators also hold a significant potential of increased average output power (or pulse energy) directly at the output of a master oscillator without any external amplification [5]. Output power achievable in F8 fibre master oscillators is predominantly limited by power handling threshold of optical elements used in the resonant cavity. Nevertheless, the highest average output powers reported earlier in mode-locked F8 fibre master oscillators reached the 100-mW level [6, 7]. The present work studied possibilities of raising substantially the output power of mode-locked F8 fibre master oscillators. Such possibilities were also indicated by the fact that fibre master oscillators based on a different configuration (mode-locked by semiconductor saturable absorbers) were successfully used to generate average output power of 2.4 W with pulse duration of 44 ps [8].

Passive mode-locking in F8 fibre master oscillators is usually achieved either by means of a non-linear optical loop mirror [1, 4, 9–11] or with the help of a non-linear amplifying loop mirror (NALM) [2–7]. A comparison of laser systems relying on these two types of loop mirrors was carried out in [12], where it was demonstrated that both non-linearity of amplifying loop mirrors and the parameters of generated pulses depend on amplification. In this context, it was interesting not only to study possibilities of boosting the output power of

#225384 - $15.00 USD Received 21 Oct 2014; accepted 17 Nov 2014; published 11 Dec 2014

F8 master oscillators with NALM, but also to map the domain of variability of temporal and spectral parameters of output pulses as the output power is varied in a broad range.

The present paper reports for the first time the results of research into an all-fibre figure-eight mode-locked Yb fibre master oscillator using NALM, capable of delivering from two output ports of its resonator more than 1 W of total output power when generating trains of double-scale pulses [13–15] with envelope width not exceeding 23 ps and filled with 200-fs sub-pulses. The output power in the studied configuration of a fibre master oscillator was only limited by the power of the available pump source amounting to 7.4 W at 978 nm.

2. Experimental setup

The layout of the studied fibre master oscillator is shown in Fig. 1. Its cavity has a figure-8 shape and uses NALM for triggering mode-locked operation. All fibres used in the master oscillator had normal dispersion within the generation spectrum.

The master oscillator cavity can be nominally considered as consisting of two parts: a passive loop only containing polarisation-maintaining fibre, and an active loop forming NALM and containing active non-polarisation-maintaining Yb-doped fibre and a birefringent fibre-optical spectral filter composed of two polarisation-maintaining fibres d1, d2 with different length and two polarisation controllers [16]. The cavity's passive и active loops are interconnected by a 2 × 2 polarisation-maintaining fibre coupler with 50/50 split ratio.

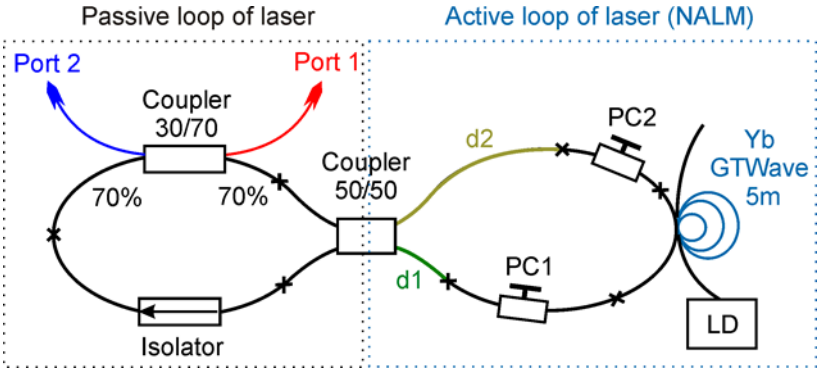

Fig. 1. Experimental layout: PC1, PC2 – polarisation controllers; LD – pump laser diode; d1, d2 – stretches of polarisation-maintaining fibre.

The passive loop of the resonator includes a fibre-optical isolator and a 2 × 2 polarisation-maintaining fibre coupler with 30/70 coupling ratio for coupling the output radiation out of the resonator. Output ratio from the exit ports of the polarisation-maintaining fibre coupler varied depending on the generation regime between 0.55 and 0.82.

The laser's gain medium was a 5-m long Yb^{3+}-doped fibre side-pumped through a coupled core-less multimode fibre (GTWave fibre assembly [17, 18]: two fibres touching sides and surrounded by a low-index cladding). Active fibre had a 10-μm core and a 125-μm cladding and had absorption of 3.9 dB/m at 978 nm. The laser was pumped with a multi-mode laser diode delivering a maximum of 7.4 W of output at 978 nm. The pigtail of the pumped laser diode was mode-matched to the coupled multimode fibre that we used to side-pump the Yb^{3+}-doped fibre. The pigtail itself was a stretch of multi-mode fibre with a 105-μm core and a 125-μm cladding.

Polarisation controllers installed close to splicing points of the standard single-mode fibre with polarisation-maintaining fibres d1 (80 cm long) and d2 (40 cm long) were used to set the radiation polarisation and to tune the fibre birefringent filter.

The master oscillator configuration studied in this work used fibre components able to withstand up to 2 W of continuous radiation.

#225384 - $15.00 USD Received 21 Oct 2014; accepted 17 Nov 2014; published 11 Dec 2014

For measurement of temporal properties of the generated pulses, we used a scanned auto-correlator FS-PS-Auto with working range of pulse durations from 10 fs to 35 ps and a fast oscilloscope/photo-detector combination with temporal resolution of 32 ps.

3. Experimental results

Depending on the configuration of the polarisation controllers and the pump power, different generation regimes could be realised, among which we identified two distinct ones with a single pulse train (cluster) over one cavity round trip and relatively stable pulse parameters. The first of these regimes (RG1) produced a wide ($\Delta\lambda$ = 0.4–5.4 nm) radiation spectrum with no more than 2% pulse-to-pulse peak power instability. Output spectrum width of the second regime (RG2) was within the range of $\Delta\lambda$ = 21–32 nm, pulse-to-pulse peak power instability reaching 30%. Figure 2 demonstrates auto-correlation functions (ACF) (Fig. 2(a)) and radiation spectra (Fig. 2(b)) of pulses generated in these two regimes at pump power of 7.4 W. It can be seen that the pulse envelope widths in these regimes are close, being equal to 21 and 23 ps, whereas their radiation spectra exhibit significant differences in width and shape (the spectrum widths differ by almost a factor of 6). The shape of the measured ACF is typical for double-scale pulses [14]: they feature a narrow (200 fs) peak on top of a picosecond-wide pedestal, although the ACF measured in different generation regimes vary in magnitude of the narrow peak by a factor of 2, indicating substantially different degree of coherence of pulses generated in different regimes [19].

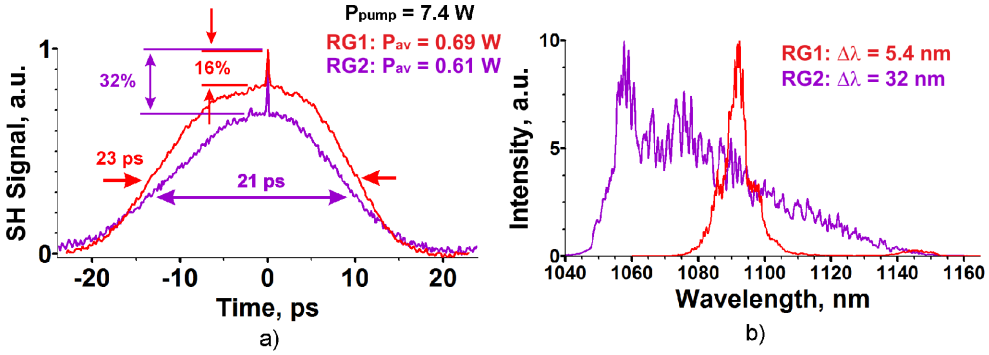

Fig. 2. (a) Auto-correlation functions and (b) radiation spectra of two typical generation regimes (RG 1 and RG 2) with one pulse train (cluster) per cavity round trip.

The larger fraction of the output was coupled through port 1 (Fig. 1) and amounted to 690 mW in regime RG 1 and 610 mW in regime RG 2 at the highest pump power of 7.4 W. As the pump power was adjusted, output radiation spectra changed considerably in both regimes (Fig. 3 and Fig. 4), however the pulse auto-correlation function underwent far less significant evolution.

The radiation spectrum of Fig. 3 exhibits both the main peak centred at 1090–1095 nm and a relatively small secondary peak located around 1140–1150 nm and corresponding to the first Stokes component of stimulated Raman scattering (SRS) in silica fibre. It should be borne in mind that wavelengths between 1140 and 1150 nm fall outside the working range of the coupler used in the master oscillator to feed radiation out of the cavity. Therefore, Fig. 3 merely indicates the presence in the cavity of the 1th Stokes pulse of SRS, not allowing a valid quantitative estimate of intensity ratio between radiation at wavelengths 1090–1095 and 1140–1150 nm. Intra-cavity conversion of the fundamental radiation into the 1th Stokes pulse of SRS in mode-locked ring fibre master oscillators was observed earlier [20, 21]. As the pumping power grows, intra-cavity Raman conversion begins limiting the intensity of the fundamental radiation component in generated pulses by channelling the intra-cavity radiation energy into multi-colour Stokes components incurring additional energy losses in the process

#225384 - $15.00 USD Received 21 Oct 2014; accepted 17 Nov 2014; published 11 Dec 2014

of SRS. Therefore, as the pump radiation intensity is further increased, the studied F8 fibre master oscillator tends to generate related multi-colour pulses, however the generated oscillator power in the first and subsequent Stokes components depends to a significant degree upon spectral parameters of the passively transmitting elements (couplers, isolator) of the studied resonator.

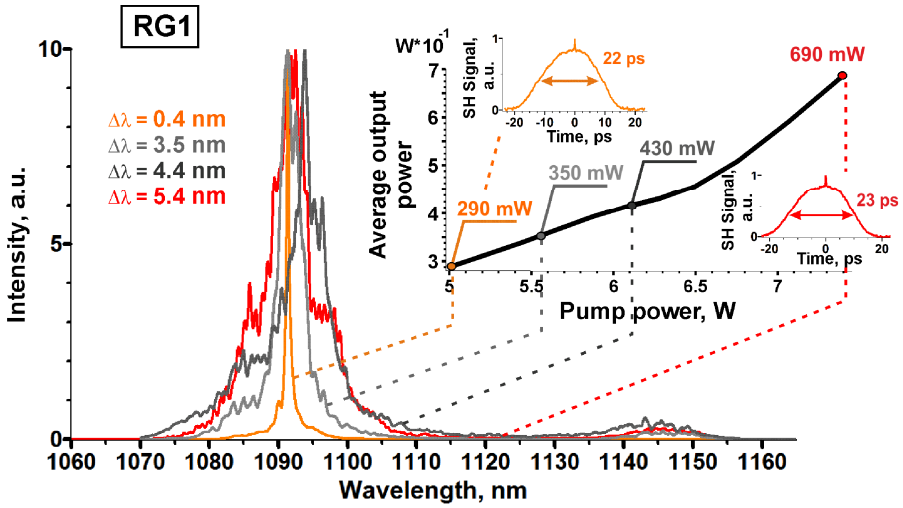

Fig. 3. Output spectrum evolution in regime RG1 versus the pump radiation power. Inset: dependence of the average output power from port 1 of the F8 master oscillator upon the pump radiation power and the shape of pulse auto-correlation function at the average output power from port 1 of the F8 master oscillator equal to 290 mW and 690 mW.

Average radiation output power from port 1 was 380 mW in regime RG1 and 500 mW in regime RG2. Therefore, the total average power of the output radiation from both ports 1 and 2 at the highest possible pump power in regime RG1 reached 1.07 W and in regime RG2, 1.11 W. Radiation spectra at the exit of ports 1 and 2 of the F8 master oscillator and dependence of the average radiation power from these ports in generation regimes RG1 and RG2 are given in Fig. 5.

Spectral width of radiation at the exit of port 2 was approximately 1.5 times larger than that of radiation from port 1, measuring 9.1 nm (RG1) and 47 nm (RG2).

Coupling of pulsed radiation out of port 2 in stationary generation notwithstanding an optical isolator inside the cavity's passive loop occurs because of a periodical transmission function of NALM with a fused polarisation-maintaining coupler [2, 3, 12, 22], which allows pulsed radiation to filter from the passive cavity loop into the active loop in both directions (both towards the optical isolator and away from it towards port 2).

#225384 - $15.00 USD Received 21 Oct 2014; accepted 17 Nov 2014; published 11 Dec 2014

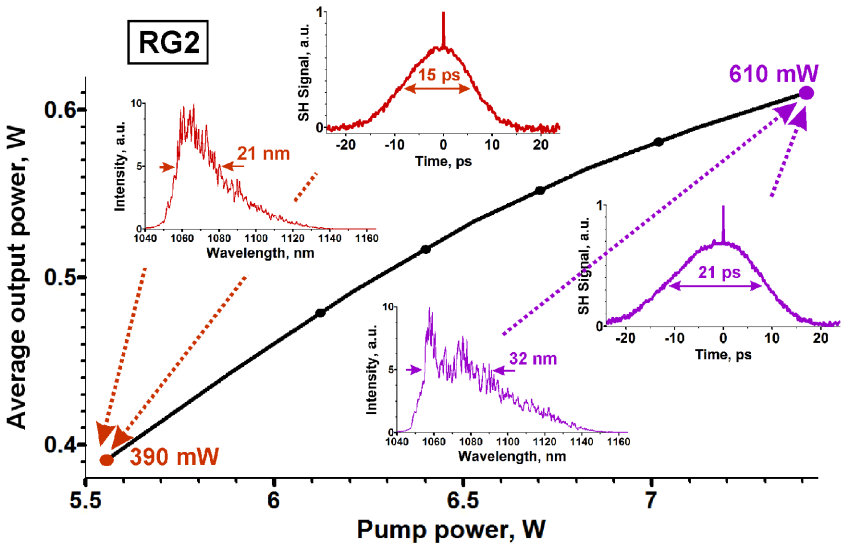

Fig. 4. Dependence upon the pump power of the average output power from port 1 of the F8 master oscillator in regime RG2. Inset: radiation spectra and auto-correlation functions of pulses at the average output power from port 1 of F8 master oscillator equal to 390 mW and 610 mW.

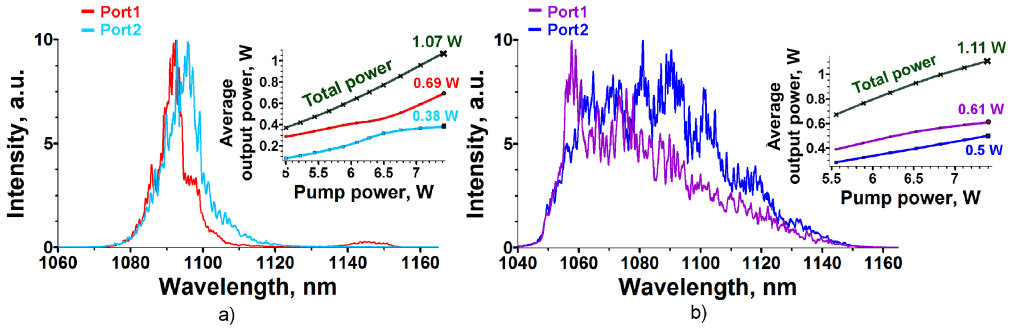

Fig. 5. (a) Spectra of radiation from ports 1 and 2 of the F8 master oscillator in generation regime RG1 (inset: dependence of average radiation power at the exit of these ports in regime RG1); (b) Spectra of radiation from ports 1 and 2 in generation regime RG2 (inset: dependence of average radiation power at the exit of these ports in regime RG2).

4. Modelling

In order to correctly interpret the obtained results, let us consider a simple model where the field or a laser double-scale pulse [14] generated in the mode-locked F8 fibre master oscillator is represented as superposition of a regular and stochastic components:

$$P(t) = \frac{1+\varepsilon(t)^2}{\cosh^2(t/T)}, \qquad (1)$$

where $P(t)$ is the dependence of radiation power on time, T – pulse duration, ε – normally distributed stochastic complex part of the pulse field. Component $\varepsilon \sim N(0,\sigma^2)$ is the result of superposition of a large number of uncorrelated modes. Under these assumptions, we can derive the expression for the magnitude ξ of the femtosecond peak on top of the picosecond pedestal of the auto-correlation function (ACF):

#225384 - $15.00 USD Received 21 Oct 2014; accepted 17 Nov 2014; published 11 Dec 2014

$$\xi = \frac{1+4\sigma^2\left(1+\sigma^2\right)}{1+8\sigma^2\left(1+\sigma^2\right)}, \qquad (2)$$

Magnitude of the femtosecond ACF peak ξ (2) monotonically increases with the fluctuation level σ, see Fig. 6(a). This leads us to expect that regime RG2 with a higher ACF peak has a larger stochastic component in generated pulses compared to regime RG1. Instantaneous transmittance T of the NALM loop is given by the expression $T = 1 - 2r(1-r)[1+\cos(\Delta\varphi)]$ [22], where $r = 0.5$ is the coupling ratio and $\Delta\varphi$ – difference in non-linear phases of counter-propagating waves. Integrating the transmittance over the pulse and averaging over the field fluctuations (1), we will obtain ratio of powers P_2 / P_1 for pulses with different magnitude ξ of the ACF peak (see Fig. 6(b)). It can be seen that the minimum of this ratio $P2/P1 = 0.36$ is reached for conventional (single-scale) pulses having a sech^2 envelope (they were not generated in the studied laser, and this case is only mentioned for the sake of comparison). As field fluctuations σ in model (1) grow, so does the minimal ratio P_2 / P_1, and oscillations on the curve P_2 / P_1 versus the average power are smoothed out because of averaging over fluctuations of radiation power inside the double-scale pulse. Predictions of model (1) qualitatively agree with the experiment: for pulses in regime RG2 with magnitude of the ACF peak $\xi = 32\%$, ratio P_2 / P_1 is close to 0.8 (Fig. 6(c)).

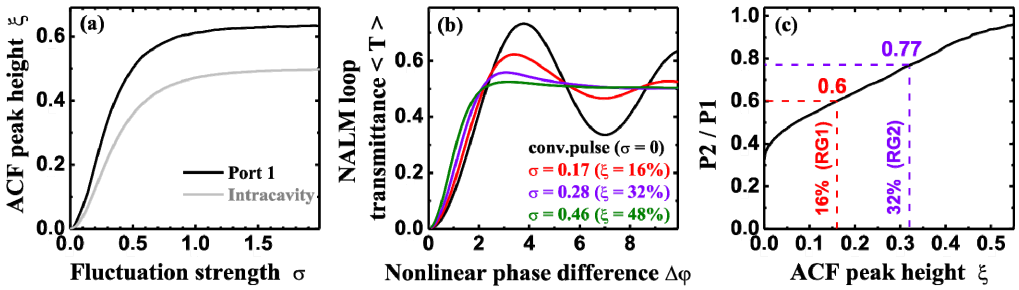

Fig. 6. Modelling results (a) ACF peak height ξ *vs.* field fluctuation strength σ; (b) time- and ensemble-averaged NALM loop transmition coeff. T; (c) power ratio P_2 / P_1 as a function of ξ.

The developed simple model of double-scale pulses (1) allows us to draw the following qualitative conclusions:

1) Minimal fraction of pulsed radiation propagating in the direction blocked by the isolator amounts to about 30% for conventional (single-scale) pulses with a sech^2 envelope.

2) For double-scale pulses, the proportion of counter-propagating (towards port 2) radiation is higher than that for conventional (single-scale) pulses and grows with the level of field fluctuations due to averaging over fluctuations of radiation power inside the pulse train (cluster).

3) For double-scale pulses with lower degree of coherence (and, therefore, a larger ACF peak height magnitude ξ), NALM loop transmittance converges to 50% for large non-linear phase difference (Fig. 6(b)).

Therefore, installation of a four-port fibre coupler after the isolator (Fig. 1) for coupling the radiation out of the cavity adds another output port for the radiation propagating in the opposite direction (that of port 2) with parameters comparable to those of the main output

#225384 - $15.00 USD Received 21 Oct 2014; accepted 17 Nov 2014; published 11 Dec 2014

radiation. The power of radiation exiting port 2 in double-scale generation regimes may equal the power of output exiting the main port 1.

5. Conclusion

The studied all-fibre figure-eight mode-locked Yb fibre master oscillator with a NALM allowed to generate the highest reported to date average radiation output power exceeding 1 W. This laser features radiation output through two ports with the ratio of the secondary port output power to the main output power varying between 0.55 and 1. Parameters of radiation exiting both ports have been experimentally measured in two distinct generation regimes, significantly differing in spectra of generated radiation. In all studied cases, the output radiation represented a sequence of pulse trains (clusters) with envelope width not exceeding 23 ps following at repetition rate of 25 MHz and stochastically filled with femtosecond sub-pulses with duration not exceeding 200 fs. It must be noted that temporal and spectral parameters of output pulses varied substantially as the output power of radiation coupled out of both ports was adjusted. A broad variability range of spectral pulse parameters in the studied F8 fibre master oscillator accompanying changes in output power is comparable with the variability range of spectral pulse parameters in a fibre master oscillator mode-locked by NPE [23], which is observed at different settings of polarisation controllers in the NPE-based mode-lock oscillator.

Output radiation power in the used configuration of fibre master oscillator was entirely limited by the available pump power of 7.4 W at 978 nm. The achieved relatively high average output radiation power and the possibility of its subsequent increase combined with certain advantages of the generated picosecond pulses (clusters of femtosecond sub-pulses) opens up new prospects of application of F8 mode-locked fibre master oscillators in many important fields, some of which have already become conventional, such as efficient non-linear transformation of radiation [24, 25], laser-induced breakdown spectroscopy [14], micromachining [26, 27], surface texturing [28], laser ablation and deposition [29], and many others.

Radiation output from two ports with broadly different spectra allows the studied laser to act as a simultaneous source of light with both narrow and broad spectra having close pulse duration. The unique combination of these output radiation parameters opens possibility of new challenges, which could be solved with a fibre-optical source of pulsed laser radiation featuring such interesting properties.

Acknowledgments

This work was supported by the Grants of Ministry of Education and Science of the Russian Federation (agreement No. 14.B25.31.0003, ZN-06-14/2419, order No. 3.162.2014/K); Russian President Grant MK-4683.2013.2; Council of the Russian President for the Leading Research Groups (project No. NSh-4447.2014.2); the Russian Foundation for Basic Research No. 14-02-31198.